Linking source and sink: The timing of deposition of Paleogene syntectonic strata in Central Asia

Feng Cheng, Andrew V Zuza, Marc Jolivet, Andreas Mulch, Niels Meijer, Zhaojie Guo

GEOLOGY | THE GEOLOGICAL SOCIETY OF AMERICA®

https://doi.org/10.1130/G51382.1

Manuscript received 15 May 2023
Revised manuscript received 22 August 2023
Manuscript accepted 30 August 2023

Published online 12 September 2023

Linking source and sink: The timing of deposition of Paleogene syntectonic strata in Central Asia

Feng Cheng[1,2,*], Andrew V. Zuza[3], Marc Jolivet[4], Andreas Mulch[2,5], Niels Meijer[2], and Zhaojie Guo[1]

[1]Key Laboratory of Orogenic Belts and Crustal Evolution, Ministry of Education, School of Earth and Space Sciences, Peking University, 100871 Beijing, China
[2]Senckenberg Biodiversity and Climate Research Centre, 60325 Frankfurt am Main, Germany
[3]Nevada Bureau of Mines and Geology, University of Nevada, Reno, Nevada 89557, USA
[4]Géosciences Rennes–UMR CNRS 6118, Université de Rennes, 35000 Rennes, France
[5]Institute of Geosciences, Goethe University Frankfurt, 60438 Frankfurt am Main, Germany

ABSTRACT

Determining the age of siliciclastic continental sequences in the absence of comprehensive biostratigraphy or radiometric dating of geological markers (e.g., volcanic layers) is inherently challenging. This issue is well exemplified in the current debate on the age of Cenozoic terrestrial strata in Central Asia, where competing age models constrained by non-unique paleomagnetic correlations are interpreted to reflect the growth of the Tibetan Plateau and its impact on Central Asian climate change. Here we present a new approach to evaluate competing age models by comparing the onset of rapid basement exhumation constrained by low-temperature thermochronology in the sediment source region with the initiation of growth strata in the adjacent sedimentary sink. We first validate this method in regions with well-constrained age models and subsequently apply this approach to the Tarim and Qaidam Basins in the northern Tibetan Plateau. The results of this analysis show that syntectonic sedimentation had already initiated during the Paleocene–Eocene and was followed by intensified Oligocene–Miocene mountain building along the northern margin of the plateau. Based on this refined Paleogene tectonic history, we further arrive at a temporal correlation between Paleogene tectonism in Northern Tibet and the retreat of the Proto-Paratethys Sea, a major water body that extended across Eurasia and was closely associated with climatic and biodiversity changes. We thus highlight the previously underestimated role tectonics in Northern Tibet had in the evolution and demise of the Proto-Paratethys Sea during the Paleogene.

INTRODUCTION

Because correlation of paleomagnetic data from continental basins to the Geomagnetic Polarity Time Scale (Ogg, 2020) is commonly non-unique, magnetostratigraphy alone can lead to dramatically different age models for continental siliciclastic sequences in the absence of fossils or radiometrically datable volcanic ash layers (Lowe, 2011). This inevitably leads to contrasting models for the timing, rates, and duration of tectonic and paleoclimatic processes. This fundamental challenge is well exemplified in Cenozoic terrestrial strata in Central Asia (Figs. 1A–1E), where competing age models have strongly diverging implications for the growth of the Tibetan Plateau (Ji et al., 2017; Staisch et al., 2020; Wang et al., 2022) and its association with Asia paleo-environments including the retreat of the Proto-Paratethys Sea, a major water body that covered large surfaces of Eurasia during the Paleogene (Bosboom et al., 2017; Sun and Liu, 2006; Zheng et al., 2015).

The two largest terrestrial basins in the Cenozoic Tibetan orogen are the Tarim and Qaidam Basins, which contain critical archives of mountain building and paleoclimate (Fig. 1B). The growth strata and thick-bedded conglomerates in the Lulehe Formation, the basal stratigraphic unit of Cenozoic strata in the Qaidam Basin (Fig. 1D), are interpreted as synorogenic sediments that record the initiation of mountain building in Northern Tibet in response to the ca. 60 Ma India-Asia collision (Ding et al., 2022; Yin et al., 2008). However, due to a lack of directly datable geologic markers and the scarcity of vertebrate fossils, two strongly contrasting age models, with a basal age of either ca. 50 Ma (Ji et al., 2017) or ca. 30 Ma (Wang et al., 2022), have been proposed for the depositional age of the Lulehe Formation, resulting in competing models for the lateral growth history of the Tibetan Plateau (Staisch et al., 2020; Wang et al., 2022; Yin et al., 2008). A similar debate centers around the depositional age of Cenozoic strata in the Tarim Basin, where some have proposed a Pliocene age for the Artux Formation (Sun and Liu, 2006) but others have assigned ages of ca. 27–15 Ma for the same unit (Zheng et al., 2015) (Fig. 1E). This differing age assignment on the eolian- and gypsum-bearing Artux Formation has led to a fundamental debate about the timing of aridification in Central Asia (Licht et al., 2016; Liu et al., 2014; Sun and Liu, 2006). In addition, knowledge about the exact timing of deposition of Lulehe Formation affects interpretations on how the Proto-Paratethys Sea retreated permanently from Central Asia (Bosboom et al., 2017; Ma et al., 2022) (Fig. 1B) and in turn impacted the regional climate and biodiversity (Barbolini et al., 2020; Meijer et al., 2019). The latter regression was attributed to the combined effect of eustatic fluctuations and far-field tectonics in response to the India-Asia collision (Bosboom et al., 2017; Burtman and Molnar, 1993; Dupont-Nivet et al., 2007; Kaya et al., 2019). However, given strikingly different interpretations depending on the age model for the deposition of syntectonic strata in the Qaidam Basin, it remains elusive whether Paleogene tectonism along Northern Tibet impacted regression in the areal extent of the Proto-Paratethys Sea.

Here we present a simple yet novel approach to assessing age models in tephra- and fossil-

Feng Cheng https://orcid.org/0000-0001-8734-6183
*cfcf.chengfeng@gmail.com

CITATION: Cheng, F., et al., 2023, Linking source and sink: The timing of deposition of Paleogene syntectonic strata in Central Asia: Geology, v. XX, p. , https://doi.org/10.1130/G51382.1

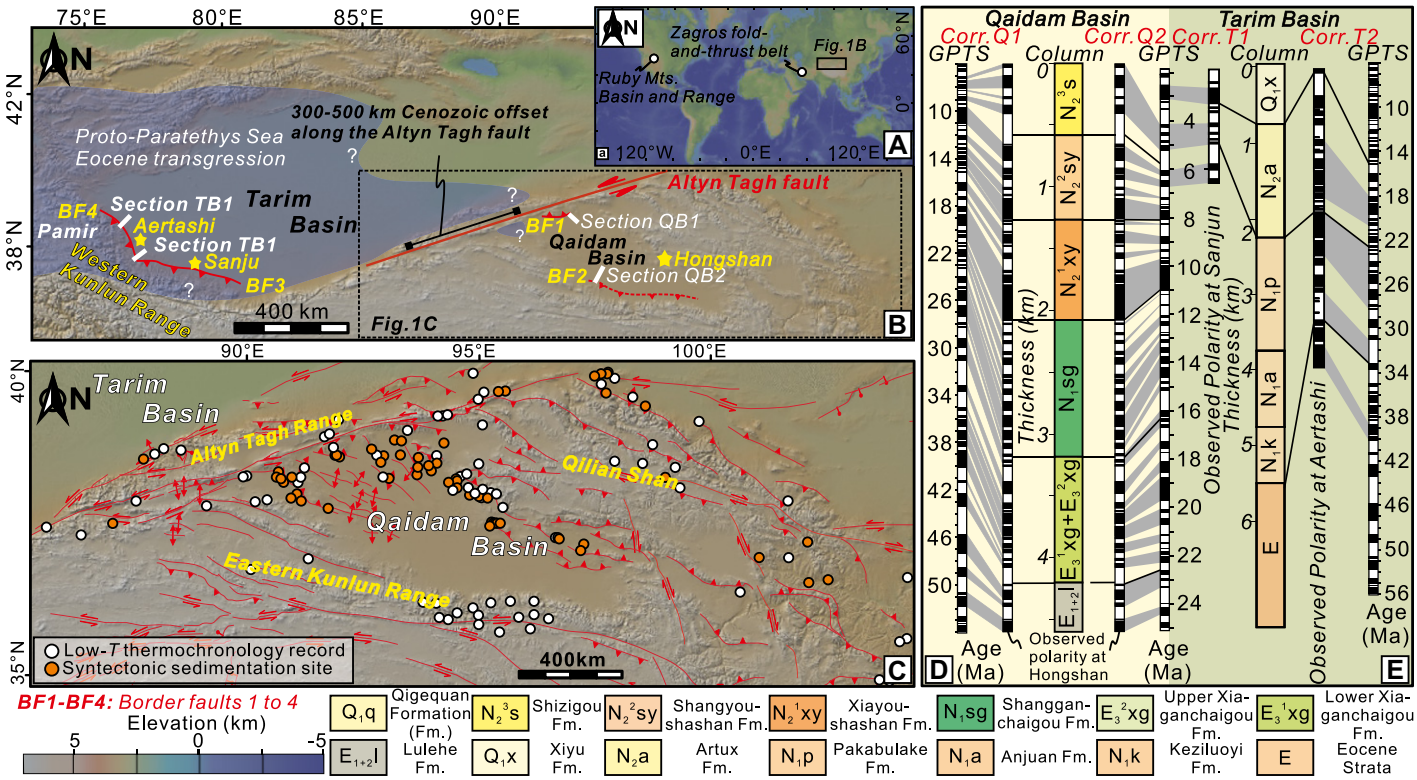

Figure 1. (A–C) Topographic maps of the globe (A), Central Asia (B), and Tibetan Plateau (C). Low-temperature (low-*T*) thermochronology and syntectonic sedimentation data are from studies listed in Table S1 (see text footnote 1). (D) Competing age models for Cenozoic strata in Qaidam Basin with basal age of either ca. 50 Ma (Q1) (Ji et al., 2017) or ca. 30 Ma (Q2) (Wang et al., 2022). (E) Competing age models for Artux Formation (Tarim Basin) with either a Pliocene–Quaternary sequence (T1) (Sun and Liu, 2006) or an Oligocene–Miocene sequence (T2) (Zheng et al., 2015). GPTS—Geomagnetic Polarity Time Scale (Ogg, 2020).

poor strata by linking source to sink of such sediments and examining the temporal relationship between rapid basement exhumation and syntectonic sedimentation. Applying this approach to the Tarim and Qaidam Basins, we constrain the depositional age of Paleogene syntectonic strata in both basins and explore the correlation between Paleogene tectonism in Northern Tibet with the regression of the Proto-Paratethys Sea.

METHODOLOGY

Magnitudes and rates of exhumation determined by low-temperature thermochronology (LTT) and growth-strata deposition provide constraints on the timing of range exhumation in and around syntectonic basins that can be interpreted to reflect major phases of fault activity. The onset timing of growth strata in the immediate vicinity of a basin-bounding fault should largely coincide with the timing of intensified exhumation linked to fault activity (Figs. 2A and 2B). Competing age models for the associated stratigraphic units can be evaluated by comparing the onset of rapid exhumation and correlative faulting revealed by LTT with the proposed age of associated growth strata defined by magnetostratigraphic correlation (Figs. 2A–2D). To validate this approach, we investigate fault activity in the Zagros fold-and-thrust belt (hereafter Zagros Mountains) in Iran and the Ruby Mountains metamorphic core complex (hereafter Ruby Mountains) in western North America (Figs. S1 and S2 in the Supplemental Material[1]), where the depositional ages of the syntectonic strata are well established by radiometric ages (Figs. 2E–2J). We then apply this approach to the Tarim and Qaidam Basins to evaluate the debated magnetostratigraphic ages of Paleogene syntectonic strata. By integrating these newly constrained Paleogene tectonism data from the Qaidam Basin with published LTT records (He et al., 2018), we explore the role of intra-plate deformation in driving the Proto-Paratethys Sea incursions. Geological background and statistical analyses of the Paleogene tectonism in Northern Tibet are given in Texts S1 and S2 in the Supplemental Material.

RESULTS AND DISCUSSION

Linkage between Syntectonic Sedimentation and Rapid Basement Exhumation

In the Zagros Mountains (Figs. 2E–2G), apatite (U-Th)/He (AHe) data from the hanging wall of the Kirkuk fault record rapid reverse-faulting exhumation at ca. 8–7 Ma (Koshnaw et al., 2020b), which is consistent with the initiation of growth strata in the footwall of the Kirkuk fault at ca. 8.0 Ma (Koshnaw et al., 2017, 2020a). In the Ruby Mountains (Figs. 2H–2J), apatite fission-track (AFT) and AHe ages from the footwall of the Ruby detachment show evidence of rapid normal-faulting exhumation at 17–15 Ma (Colgan et al., 2010), coinciding with the initiation of growth strata in the hanging wall of the detachment at ca. 16 Ma (Lund Snee et al., 2016; Satarugsa and Johnson, 2000). These consistencies between the rapid exhumation and basement cooling in the source area and the initiation of growth strata in the associated sedimentary sink lend strong support to the proposed age model of the late Cenozoic strata in the Zagros and Ruby Mountains, allowing us to apply this approach to debated stratigraphic age models in Central Asia.

Age Models for the Strata in the Qaidam and Tarim Basins and Implications for Intraplate Deformation

In the northwestern Qaidam Basin, AFT data from the basement rocks in the hanging wall of fault BF1 show rapid exhumation at 50–30 Ma and 30–10 Ma (Fig. 3A). These time intervals are widely interpreted as evidence for a two-stage rock uplift of the Altyn Tagh Range (Jolivet

[1]Supplemental Material. Texts S1–S4, Figures S1–S4, and Table S1. Please visit https://doi.org/10.1130/GEOL.S.24069507 to access the supplemental material, and contact editing@geosociety.org with any questions.

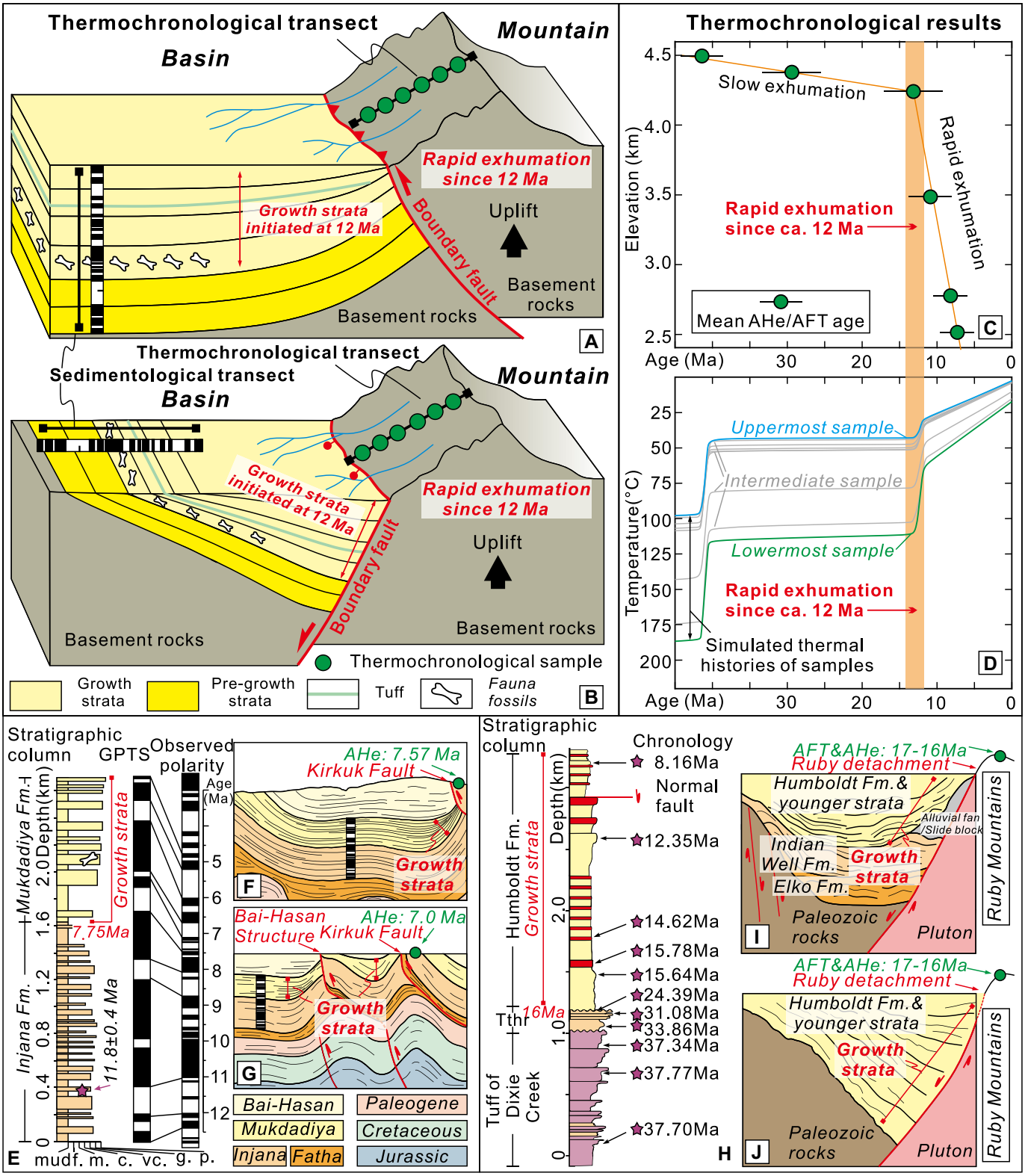

Figure 2. (A, B) Hypothetical sedimentary sequence with contrasting interpretations of magnetostratigraphic ages is deposited in basin with either reverse (A) or normal (B) fault bounding basement undergoing exhumation. Exhumed material is deposited within growth strata of the sedimentary sequence. (C, D) Timing of growth strata can be compared with thermochronology data recording onset of exhumation. Error bars represent one standard deviation of uncertainty. (E–G) Based on magnetostratigraphy (E), initiation of growth strata shown on seismic profiles across the Zagros (Iran) was dated at ca. 8 Ma (Koshnaw et al., 2020a; Koshnaw et al., 2017), coeval with the onset of basement uplift at ca. 8–7 Ma recorded by thermochronology (Koshnaw et al., 2020b) (F, G). Abbreviations f., m., c., vc., g., and p. represent fine-grained, medium-grained, coarse-grained, very coarse-grained, granule, and pebble, respectively; Tthr represents Oligocene tuff of Hackwood Ranch and underlying sedimentary rocks. The red horizons represent volcanic ash layers. (H–J) Dated tuffs (Lund Snee et al., 2016) (H) and seismic profiles (Satarugsa and Johnson, 2000) (I, J) from the Ruby Mountains (western North America) show growth strata starting at 16 Ma, coeval with 17–15 Ma age recorded by thermochronology (Colgan et al., 2010). Locations of profiles are shown in Figures S1 and S2 (see text footnote 1). AHe—apatite (U-Th)/He; AFT—apatite fission-track; GPTS—Geomagnetic Polarity Time Scale (Ogg, 2020).

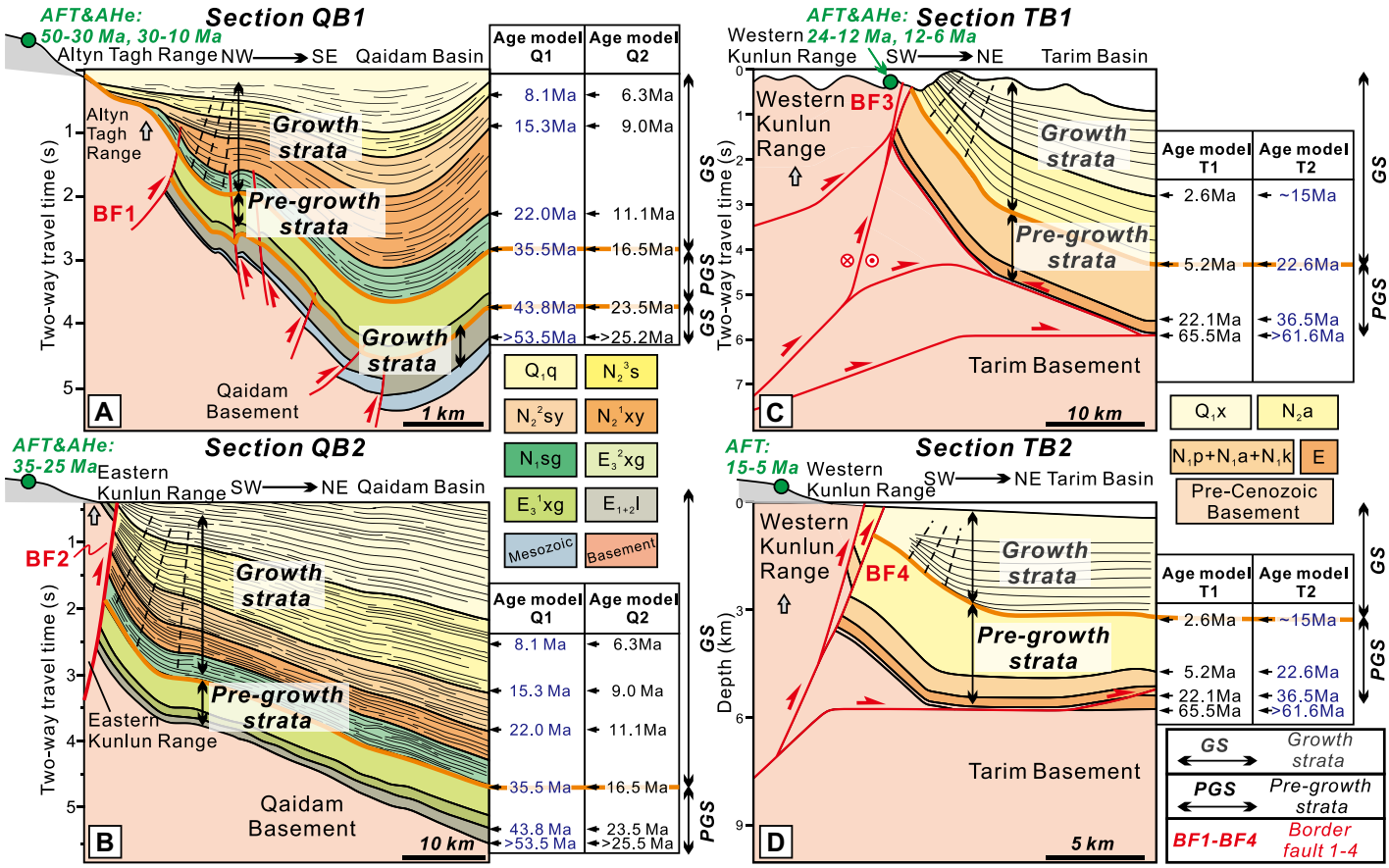

Figure 3. Seismic profiles in northwestern (A) and southern (B) Qaidam Basin (Cheng et al., 2021) and southwestern Tarim Basin (C, D) (Wang and Wang, 2016), showing growth strata in response to rock uplift of the Altyn Tagh, Eastern Kunlun, and Western Kunlun Ranges. Locations are shown in Figure 1B. Preferred age model is in orange. The age models Q1, Q2, T1, and T2 are from Ji et al. (2017), Wang et al. (2022), Sun et al. (2006), and Zheng et al. (2015), respectively. AFT—apatite fission-track; AHe—apatite (U-Th)/He; GS—growth strata; PGS—pre-growth strata. $E_1 + {}_2l$, $E_3{}^1xg$, $E_3{}^2xg$, N_1sg, $N_2{}^1xy$, $N_2{}^2sy$, $N_2{}^3S$, and Q_1q are abbreviations for Lulehe, Lower Xiaganchaigou, Upper Xiaganchaigou, Shanganchaigou, Xiayoushashan, Shangyoushashan, Shizigou, and Qigequan formations, respectively. E, N_1p, $N_1a + N_1k$, N2a, and Q_1x are the abbreviations for Eocene strata, Pakabulake + Anjuan + Keziluoyi, Artux, and Xiyu formations, respectively.

et al., 2001; Zhang et al., 2012). As shown on section QB1 (Fig. 3A), two sequences of growth structures occur in the footwall of fault BF1 that are consistent with pulsed exhumation of the basement (Cheng et al., 2021). Following age model Q1 (Ji et al., 2017), the growth strata indicate rock uplift and basement exhumation during the Paleocene–Eocene and Oligocene–Miocene, respectively. This is consistent with the exhumation history of the Altyn Tagh basement revealed by LTT. However, following age model Q2 (Wang et al., 2022), the growth strata indicate pulsed rock uplift at >25.5–23.5 Ma and 16.5 to <6.3 Ma, separated by tectonic quiescence from 23.5 Ma to 16.5 Ma. This second scenario contradicts the Miocene exhumation of the Altyn Tagh basement indicated by LTT data (Jolivet et al., 2001; Zhang et al., 2012).

In the southern Qaidam Basin, AFT and AHe data from the basement on the hanging wall of fault BF2 (Fig. 3B) show rapid exhumation at ca. 35–25 Ma, indicating rapid exhumation of the Eastern Kunlun Range from the latest Eocene to Oligocene (Clark et al., 2010; Li et al., 2021). Growth strata (section QB2, Fig. 3B) are developed in the footwall of fault BF2 (Cheng et al., 2021), suggesting a corresponding rock uplift and exhumation of the Eastern Kunlun Range. Following age model Q1, the occurrence of the growth strata indicates rapid rock uplift and exhumation of the Eastern Kunlun basement from 35.5 to <8.1 Ma, consistent with the exhumation history of the Eastern Kunlun basement revealed by LTT. However, following age model Q2, the resulting age of the growth strata requires tectonic quiescence from >25.5 Ma to 16.5 Ma with subsequent rapid rock uplift from 16.5 to <6.3 Ma. This second scenario contradicts the recognized latest Eocene–Oligocene rapid exhumation of the Eastern Kunlun basement.

In the southwestern Tarim Basin (section TB1, Fig. 3C), AFT data from the hanging wall of fault BF3 reveal rapid exhumation at 24–12 Ma and 12–6 Ma, which are interpreted as evidence of two-stage rock uplift of the Western Kunlun Range (Li et al., 2019). Corresponding growth structures are observed on the footwall of fault BF3 (Wang and Wang, 2016) (Fig. 3C). Following age model T1 (Sun and Liu, 2006), the growth strata indicate a prolonged tectonic quiescence period from 65.5 Ma to 5.2 Ma, with rapid rock uplift of the basement occurring during the Pliocene (>5.2 Ma to <2.6 Ma). This contradicts the proposed late Oligocene to Miocene rapid exhumation of the Western Kunlun Range based on LTT data. However, following age model T2 (Zheng et al., 2015), the growth strata suggest rapid faulting initiation along fault BF3 at ca. 22.6 Ma, consistent with the LTT record. Moreover, in section TB2 (Fig. 3D), AFT data from the hanging wall of fault BF4 show rapid exhumation and rock uplift of the Western Kunlun Range at 15–5 Ma (Cao et al., 2015). Growth strata are well preserved in the footwall of fault BF4. Following age model T1 (Sun and Liu, 2006), the pre-growth strata indicate prolonged tectonic quiescence from 65.5 Ma to 2.6 Ma while the growth strata suggest the onset of rapid rock uplift of the Western Kunlun Range at ca. 2.6 Ma (Fig. 3D). This scenario contradicts the Miocene to Pliocene rapid exhumation of the Western Kunlun Range derived from LTT data (Cao et al., 2015). However, following age model T2, the growth strata indicate a ca. 15 Ma

initiation of rapid faulting, consistent with the exhumation history of the Western Kunlun basement based on LTT.

The inconsistency between the LTT data in exhuming source regions and the age of growth-strata relationships in the adjacent sedimentary basins reveals that both "young" age models (Q2 and T1) for Cenozoic strata in the Qaidam and Tarim Basins, while magnetostratigraphically reasonable, are in conflict with the exhumation history of surrounding basement units. Our analysis hence indicates that the timing of syntectonic sedimentation is in very good agreement with age models Q1 and T2. Sedimentation initiated during the Paleocene–Eocene and was followed by intensified Oligocene–Miocene mountain building along the northern Tibetan Plateau margin. This episodic mountain building along the northern margin of the Tibetan Plateau highlights key features of out-of-sequence intra-plate deformation promoted by the post-collisional convergence.

Did Paleogene Tectonism in Northern Tibet affect Proto-Paratethys Sea Retreat?

Because Paleogene marine incursions in the Tarim Basin do not simply align with eustatic sea-level changes (Figs. 4A–4C), recent studies have suggested a dominant role of tectonic loading and basin filling associated with the growth of the Pamir salient in the Proto-Paratethys Sea evolution (Kaya et al., 2019). However, Paleogene marine records were recently discovered farther east in the Qaidam Basin (Ma et al., 2022) indicating that the Proto-Paratethys Sea extended into Northern Tibet, which would have been located closer to the Tarim Basin, given the 300–500 km left-lateral offset along the Altyn Tagh fault since the Eocene (Cheng et al., 2016) (Texts S3 and S4; Fig. S4). As a result, Paleogene intracontinental deformation and associated modification in surface elevations along the northern Tibetan Plateau margin could have played a crucial role in driving the Proto-Paratethys Sea retreat in addition to deformation in the Pamir (Kaya et al., 2019). However, this hypothesis remains ambiguous due to the limited LTT data in Northern Tibet (Jepson et al., 2021) and the competing age models of syntectonic strata in the Qaidam Basin.

Here we combine the newly constrained depositional age data from the Qaidam Basin with published LTT data sets, which together reflect Paleogene tectonic activity in Northern Tibet. We observe a consistent temporal correlation between tectonic activity and Proto-Paratethys Sea incursions (Figs. 4A–4D). Specifically, periods of tectonic quiescence in Northern Tibet at 57–56 Ma, 48–41 Ma, and 39–36 Ma correspond to the timing of the first, second, and third incursions of the Proto-Paratethys Sea, while peaks in tectonic activity at 56–48 Ma and 41–39 Ma coincide with the first, second, and third regressions (Fig. 4D). We propose that renewed acceleration of deformation in Northern Tibet and associated surface-elevation change promoted the intermittent retreat of the Proto-Paratethys Sea, while intervening deceleration of tectonic deformation facilitated Proto-Paratethys Sea incursions.

The temporal coincidence between tectonism in Northern Tibet and Proto-Paratethys Sea regression highlights the previously underestimated role of tectonics in Northern Tibet in the retreat of the vast marine domain through uplift and basin infilling, which together with the northward indentation of the Pamir salient as well as the global sea-level fall during the Eocene-Oligocene transition (Kaya et al., 2019), led to the demise of the Proto-Paratethys Sea in Central Asia.

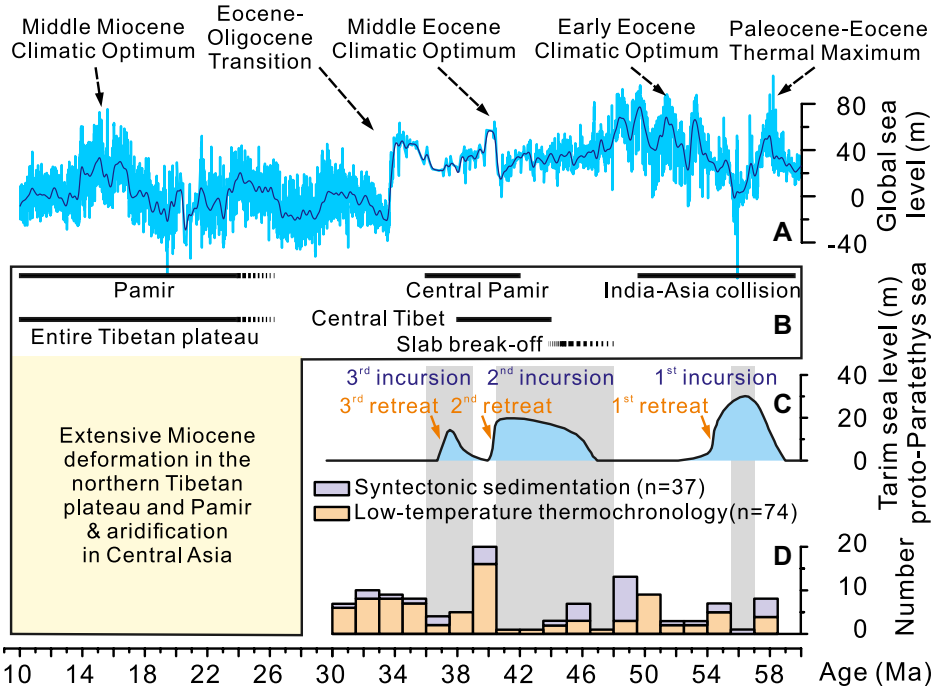

Figure 4. (A) Global sea level (Miller et al., 2020). (B) Cenozoic tectonism in Tibet and Pamir (Kaya et al., 2019). (C) Tarim sea-level fluctuation (Kaya et al., 2019). (D) Histogram of timing of tectonism in Northern Tibet. Global sea level refers to the height of the ocean's surface relative to land and averaged over the globe, while the Tarim sea level is relative to the Tarim basin. Source of tectonism is given in Table S1 (see text footnote 1).

ACKNOWLEDGMENTS

This work was supported by the National Natural Science Foundation of China (U22B6002, 41888101, 41930213) and the Alexander von Humboldt Foundation. We thank editor Robert Holdsworth, Devon Orme, Ryan Leary, and an anonymous reviewer for constructive feedback that improved the manuscript.

REFERENCES CITED

Barbolini, N., et al., 2020, Cenozoic evolution of the steppe-desert biome in Central Asia: Science Advances, v. 6, https://doi.org/10.1126/sciadv.abb8227.

Bosboom, R., Mandic, O., Dupont-Nivet, G., Proust, J.-N., Ormukov, C., and Aminov, J., 2017, Late Eocene palaeogeography of the proto-Paratethys Sea in Central Asia (NW China, southern Kyrgyzstan and SW Tajikistan), *in* Brunet, M.-F., et al., eds., Geological Evolution of Central Asian Basins and the Western Tien Shan Range: Geological Society, London, Special Publication 427, p. 565–588, https://doi.org/10.1144/SP427.11.

Burtman, V.S., and Molnar, P., 1993, Geological and Geophysical Evidence for Deep Subduction of Continental Crust Beneath the Pamir: Geological Society of America Special Paper 281, 76 p., https://doi.org/10.1130/SPE281.

Cao, K., Wang, G.C., Bernet, M., van der Beek, P., and Zhang, K.X., 2015, Exhumation history of the West Kunlun Mountains, northwestern Tibet: Evidence for a long-lived, rejuvenated orogen: Earth and Planetary Science Letters, v. 432, p. 391–403, https://doi.org/10.1016/j.epsl.2015.10.033.

Cheng, F., Jolivet, M., Fu, S.T., Zhang, C.H., Zhang, Q.Q., and Guo, Z.J., 2016, Large-scale displacement along the Altyn Tagh Fault (North Tibet) since its Eocene initiation: Insight from detrital zircon U-Pb geochronology and subsurface data: Tectonophysics, v. 677–678, p. 261–279, https://doi.org/10.1016/j.tecto.2016.04.023.

Cheng, F., Jolivet, M., Guo, Z.J., Wang, L., Zhang, C.H., and Li, X.Z., 2021, Cenozoic evolution of the Qaidam basin and implications for the growth of the northern Tibetan plateau: A review: Earth-Science Reviews, v. 220, https://doi.org/10.1016/j.earscirev.2021.103730.

Clark, M.K., Farley, K.A., Zheng, D.W., Wang, Z.C., and Duvall, A.R., 2010, Early Cenozoic faulting of the northern Tibetan Plateau margin from apatite (U-Th)/He ages: Earth and Planetary Science Letters, v. 296, p. 78–88, https://doi.org/10.1016/j.epsl.2010.04.051.

Colgan, J.P., Howard, K.A., Fleck, R.J., and Wooden, J.L., 2010, Rapid middle Miocene extension and unroofing of the southern Ruby Mountains, Nevada: Tectonics, v. 29, TC6022, https://doi.org/10.1029/2009TC002655.

Ding, L., Kapp, P., Cai, F.L., Garzione, C.N., Xiong, Z.Y., Wang, H.Q., and Wang, C., 2022, Timing and mechanisms of Tibetan Plateau uplift: Nature Reviews Earth & Environment, v. 3, p. 652–667, https://doi.org/10.1038/s43017-022-00318-4.

Dupont-Nivet, G., Krijgsman, W., Langereis, C.G., Abels, H.A., Dai, S., and Fang, X.M., 2007, Tibetan plateau aridification linked to global cooling at the Eocene–Oligocene transition: Nature, v. 445, p. 635–638, https://doi.org/10.1038/nature05516.

He, P.J., Song, C.H., Wang, Y.D., Meng, Q.Q., Chen, L.H., Yao, L.J., Huang, R.H., Feng, W., and Chen, S., 2018, Cenozoic deformation history of the Qilian Shan (northeastern Tibetan Plateau) constrained by detrital apatite fission-track thermochronology in the northeastern Qaidam Basin: Tectonophysics, v. 749, p. 1–11, https://doi.org/10.1016/j.tecto.2018.10.017.

Jepson, G., Carrapa, B., Gillespie, J., Feng, R., DeCelles, P.G., Kapp, P., Tabor, C.R., and Zhu, J., 2021, Climate as the great equalizer of continental-scale erosion: Geophysical Research Letters, v. 48, https://doi.org/10.1029/2021GL095008.

Ji, J.L., Zhang, K.X., Clift, P.D., Zhuang, G.S., Song, B.W., Ke, X., and Xu, Y.D., 2017, High-resolution magnetostratigraphic study of the Paleogene-Neogene strata in the Northern Qaidam Basin: Implications for the growth of the Northeastern Tibetan Plateau: Gondwana Research, v. 46, p. 141–155, https://doi.org/10.1016/j.gr.2017.02.015.

Jolivet, M., Brunel, M., Seward, D., Xu, Z., Yang, J., Roger, F., Tapponnier, P., Malavieille, J., Arnaud, N., and Wu, C., 2001, Mesozoic and Cenozoic tectonics of the northern edge of the Tibetan plateau: Fission-track constraints: Tectonophysics, v. 343, p. 111–134, https://doi.org/10.1016/S0040-1951(01)00196-2.

Kaya, M.Y., et al., 2019, Paleogene evolution and demise of the proto-Paratethys Sea in Central Asia (Tarim and Tajik basins): Role of intensified tectonic activity at ca. 41 Ma: Basin Research, v. 31, p. 461–486, https://doi.org/10.1111/bre.12330.

Koshnaw, R.I., Horton, B.K., Stockli, D.F., Barber, D.E., Tamar-Agha, M.Y., and Kendall, J.J., 2017, Neogene shortening and exhumation of the Zagros fold-thrust belt and foreland basin in the Kurdistan region of northern Iraq: Tectonophysics, v. 694, p. 332–355, https://doi.org/10.1016/j.tecto.2016.11.016.

Koshnaw, R.I., Horton, B.K., Stockli, D.F., Barber, D.E., and Tamar-Agha, M.Y., 2020a, Sediment routing in the Zagros foreland basin: Drainage reorganization and a shift from axial to transverse sediment dispersal in the Kurdistan region of Iraq: Basin Research, v. 32, p. 688–715, https://doi.org/10.1111/bre.12391.

Koshnaw, R.I., Stockli, D.F., Horton, B.K., Teixell, A., Barber, D.E., and Kendall, J.J., 2020b, Late Miocene deformation kinematics along the NW Zagros fold-thrust belt, Kurdistan region of Iraq: Constraints from apatite (U-Th)/He thermochronometry and balanced cross sections: Tectonics, v. 39, https://doi.org/10.1029/2019TC005865.

Li, C.P., Zheng, D.W., Zhou, R.J., Yu, J.X., Wang, Y.Z., Pang, J.Z., Wang, Y., Hao, Y.Q., and Li, Y.J., 2021, Late Oligocene tectonic uplift of the East Kunlun Shan: Expansion of the northeastern Tibetan Plateau: Geophysical Research Letters, v. 48, https://doi.org/10.1029/2020GL091281.

Li, G.W., Sandiford, M., Fang, A.M., Kohn, B., Sandiford, D., Fu, B.H., Zhang, T.L., Cao, Y.Y., and Chen, F., 2019, Multi-stage exhumation history of the West Kunlun orogen and the amalgamation of the Tibetan Plateau: Earth and Planetary Science Letters, v. 528, https://doi.org/10.1016/j.epsl.2019.115833; corrigendum available at https://doi.org/10.1016/j.epsl.2019.115937.

Licht, A., Dupont-Nivet, G., Pullen, A., Kapp, P., Abels, H.A., Lai, Z., Guo, Z., Abell, J., and Giesler, D., 2016, Resilience of the Asian atmospheric circulation shown by Paleogene dust provenance: Nature Communications, v. 7, https://doi.org/10.1038/ncomms12390.

Liu, W.G., Liu, Z.H., An, Z.S., Sun, J.M., Chang, H., Wang, N., Dong, J.B., and Wang, H.Y., 2014, Late Miocene episodic lakes in the arid Tarim Basin, western China: Proceedings of the National Academy of Sciences of the United States of America, v. 111, p. 16,292–16,296, https://doi.org/10.1073/pnas.1410890111.

Lowe, D.J., 2011, Tephrochronology and its application: A review: Quaternary Geochronology, v. 6, p. 107–153, https://doi.org/10.1016/j.quageo.2010.08.003.

Lund Snee, J.-E., Miller, E.L., Grove, M., Hourigan, J.K., and Konstantinou, A., 2016, Cenozoic paleogeographic evolution of the Elko Basin and surrounding region, northeast Nevada: Geosphere, v. 12, p. 464–500, https://doi.org/10.1130/GES01198.1.

Ma, J., Wu, C.D., Uveges, B.T., Ding, W.M., Summons, R.E., and Cui, X.Q., 2022, Biomarkers reveal Eocene marine incursions into the Qaidam Basin, north Tibetan Plateau: Organic Geochemistry, v. 166, https://doi.org/10.1016/j.orggeochem.2022.104380.

Meijer, N., et al., 2019, Central Asian moisture modulated by proto-Paratethys Sea incursions since the early Eocene: Earth and Planetary Science Letters, v. 510, p. 73–84, https://doi.org/10.1016/j.epsl.2018.12.031.

Miller, K.G., Browning, J.V., Schmelz, W.J., Kopp, R.E., Mountain, G.S., and Wright, J.D., 2020, Cenozoic sea-level and cryospheric evolution from deep-sea geochemical and continental margin records: Science Advances, v. 6, https://doi.org/10.1126/sciadv.aaz1346.

Ogg, J.G., 2020, Geomagnetic Polarity Time Scale, *in* Gradstein, F.M., Ogg, J.G., Schmitz, M.D., and Ogg, G.M., eds., Geologic Time Scale 2020: Amsterdam, Elsevier, p. 159–192, https://doi.org/10.1016/B978-0-12-824360-2.00005-X.

Satarugsa, P., and Johnson, R.A., 2000, Cenozoic tectonic evolution of the Ruby Mountains metamorphic core complex and adjacent valleys, northeastern Nevada: Rocky Mountain Geology, v. 35, p. 205–230, https://doi.org/10.2113/35.2.205.

Staisch, L.M., Niemi, N.A., Clark, M.K., and Chang, H., 2020, The Cenozoic evolution of crustal shortening and left-lateral shear in the central East Kunlun Shan: Implications for the uplift history of the Tibetan Plateau: Tectonics, v. 39, https://doi.org/10.1029/2020TC006065.

Sun, J.M., and Liu, T.S., 2006, The age of the Taklimakan Desert: Science, v. 312, p. 1621, https://doi.org/10.1126/science.1124616.

Wang, W.T., Zhang, P.Z., Garzione, C.N., Liu, C.C., Zhang, Z.Q., Pang, J.Z., Wang, Y.Z., Zheng, D.W., Zheng, W.J., and Zhang, H.P., 2022, Pulsed rise and growth of the Tibetan Plateau to its northern margin since ca. 30 Ma: Proceedings of the National Academy of Sciences of the United States of America, v. 119, https://doi.org/10.1073/pnas.2120364119.

Wang, Z., and Wang, X., 2016, Late Cenozoic deformation sequence of a thrust system along the eastern margin of Pamir, northwest China: Acta Geologica Sinica (English Edition), v. 90, p. 1664–1678, https://doi.org/10.1111/1755-6724.12809.

Yin, A., Dang, Y.Q., Zhang, M., Chen, X.H., and McRivette, M.W., 2008, Cenozoic tectonic evolution of the Qaidam basin and its surrounding regions (Part 3): Structural geology, sedimentation, and regional tectonic reconstruction: Geological Society of America Bulletin, v. 120, p. 847–876, https://doi.org/10.1130/B26232.1.

Zhang, Z.C., Guo, Z.J., Li, J.F., and Tang, W.H., 2012, Mesozoic and Cenozoic uplift-denudation along the Altyn Tagh fault, northwestern China: Constraints from apatite fission track data: Quaternary Sciences, v. 32, p. 499–509.

Zheng, H.B., Wei, X.C., Tada, R., Clift, P.D., Wang, B., Jourdan, F., Wang, P., and He, M.Y., 2015, Late Oligocene–early Miocene birth of the Taklimakan Desert: Proceedings of the National Academy of Sciences of the United States of America, v. 112, p. 7662–7667, https://doi.org/10.1073/pnas.1424487112.

Printed in the USA